frontiers | Frontiers in Astronomy and Space Sciences

TYPE Review
PUBLISHED 11 June 2025
DOI 10.3389/fspas.2025.1608411

OPEN ACCESS

EDITED BY
Ivan Kotov,
Brookhaven National Laboratory (DOE),
United States

REVIEWED BY
Mario Gai,
Osservatorio Astrofisico di Torino (INAF), Italy
Rishikesh Kulkarni,
Indian Institute of Technology Guwahati, India
Etienne Lyard,
University of Geneva, Switzerland

*CORRESPONDENCE
Steve B. Howell,
steve.b.howell@nasa.gov

RECEIVED 08 April 2025
ACCEPTED 05 May 2025
PUBLISHED 11 June 2025

CITATION
Howell SB, Martínez-Vázquez CE, Furlan E, Scott NJ, Matson RA, Littlefield C, Clark CA, Lester KV, Hartman ZD, Ciardi DR and Deveny SJ (2025) Nearly a decade of groundbreaking speckle interferometry at the international Gemini observatory. *Front. Astron. Space Sci.* 12:1608411. doi: 10.3389/fspas.2025.1608411

Nearly a decade of groundbreaking speckle interferometry at the international Gemini observatory

Steve B. Howell[1]*, Clara E. Martínez-Vázquez[2], Elise Furlan[3], Nicholas J. Scott[4], Rachel A. Matson[5], Colin Littlefield[1,6], Catherine A. Clark[3], Kathryn V. Lester[7], Zachary D. Hartman[1], David R. Ciardi[3] and Sarah J. Deveny[1,6]

[1]Astrophysics and Space Science, NASA Ames Research Center, Moffett Field, CA, United States, [2]International Gemini Observatory/NSF NOIRLab, Hilo, HI, United States, [3]NASA Exoplanet Science Institute, Caltech/IPAC, Pasadena, CA, United States, [4]The CHARA Array, Mt. Wilson, CA, United States, [5]U.S. Naval Observatory, Washington, DC, United States, [6]Bay Area Environmental Research Institute, Moffett Field, CA, United States, [7]Department of Astronomy, Mount Holyoke College, South Hadley, MA, United States

Since its inception, speckle interferometry has revolutionized high-resolution astronomical imaging, overcoming atmospheric challenges to achieve the diffraction limits of telescopes. Almost a decade ago, in 2018, a pair of speckle cameras – 'Alopeke and Zorro–were installed at two of the largest apertures in the world, the twin 8.1-m Gemini North and South telescopes in Hawai'i and Chile. Equipped with dual blue and red channels, 'Alopeke and Zorro deliver high-resolution imaging across the optical bandpass from 350 to 1,000 nm, which has led to crucial discoveries in both stellar multiplicity and exoplanetary science. Furthermore, the broad and nonrestrictive access to these instruments, given by each Gemini Observatory partner and via the US NOIRLab open skies policy, has allowed the community to expand the applications of the instruments, supporting a wide range of scientific investigations from Solar System bodies, to morphological studies of stellar remnants and quasars, to evolved stars, to transient phenomena. This paper reviews the instrument technology and observational capabilities, and highlights key scientific contributions and discoveries of 'Alopeke and Zorro, emphasizing the enduring importance of speckle interferometry in advancing modern observational astronomy and expanding the frontiers of astronomical research.

KEYWORDS

binary stars, planet hosting stars, speckle interferometry, astronomical techniques, high angular resolution

1 Introduction

Speckle interferometry, as a technique for high-resolution optical imaging, began in 1970 with the work of Labeyrie (1970), using ideas for fast imaging to remove atmospheric effects. Labeyrie (1970) showed that taking short exposures removed the effects of seeing-induced fluctuations that were causing distortions in the wavefront from a distant star. Removing these distortions allowed the diffraction limit of the telescope to be reached.

Speckle cameras initially used photographic plates, but continued with the various detectors of the day, such as photomultiplier tubes, video tubes, and reticons (e.g., Bonneau and Foy, 1980; McAlister et al., 1987; Weigelt and Baier, 1985; Horch et al., 1992; Balega et al., 1993). Initial studies mainly focused on bright binary stars using 1- to 4-m telescopes and repeated imaging to produce precise stellar orbits (e.g., McAlister et al., 1989). Significant advances in astronomical detectors, in particular the more quantum efficient charge-coupled devices (CCDs), provided the next leap forward in this field, allowing for photon intensification, digital outputs, and higher signal-to-noise (S/N) observations to be obtained (e.g., McAlister et al., 1989; Mason et al., 1997; Hartkopf et al., 2000; Horch et al., 2000). In recent years, the introduction of the electron-multiplying CCD (EMCCD) as a detector (Tokovinin and Cantarutti, 2008; Horch et al., 2011) has been a game-changer. With ultra-fast readout, essentially zero read noise, near-perfect Quantum efficiency (QE), optical flatness, and ease of use, EMCCDs have revolutionized the field of speckle imaging. Fourier-based data reduction and image reconstructions using autocorrelation and power spectra techniques (Horch et al., 2012; Horch et al., 2015) are enhanced using the bispectrum technique developed by Weigelt (1977) and Lohmann et al. (1983) allowing phase information to be determined that resolves the ambiguity present in autocorrelation analysis (e.g., Howell et al., 2011; Hope et al., 2022).

This renaissance in speckle imaging has led to the development of new dedicated speckle instruments (e.g., Maksimov et al., 2009; Tokovinin et al., 2010; Howell et al., 2021b; Clark et al., 2020; Pedichini et al., 2016) placed on some of the largest telescopes in the world. A summary of former and current speckle imagers in astronomy is presented in Scott et al. (2021). Speckle imaging is no longer limited to bright star astrometry; it has expanded into many areas of point source and non-point source imagery (e.g., Salinas et al., 2020; Scott et al., 2021; Shara et al., 2022). Fainter astronomical targets can now be observed (Howell et al., 2021a), the overall data quality and S/N ratio of the observations are greater, and the final reconstructed images have more fidelity (e.g., Howell and Furlan, 2022).

In contrast to infrared (IR) adaptive optics (AO) systems, optical speckle imaging on 8-m-class telescopes routinely achieves an inner working angle (IWA) at the diffraction limit of the telescope (20–30 mas across the optical Lester et al., 2021), uses far less expensive instrumentation, and does not require a (laser) guide star, enabling higher observational efficiency. In speckle interferometry, the detection contrast is proportional to $1/(\text{seeing})^2$ but the angular resolution is unaffected (λ/D). This is in contrast to normal imaging and IR/AO in which the final image resolution is affected by the native seeing, being proportional to λ/r_0 (r_0 ~ native seeing, Fried, 1966). Speckle imaging performed in the optical bandpass (350–1,000 nm) provides the highest angular resolution available today on any single telescope, delivering ~4 times better angular resolution than IR AO observations in the *K*-band.

This paper presents a summary of the first 8 years of astronomical imaging observations using the highest resolution, deepest contrast speckle instruments available, ʻAlopeke and Zorro, which are mounted on the twin 8.1-m Gemini North and South telescopes in Hawai'i and Chile (Scott et al., 2021; Howell and Furlan, 2022). We review the major advances and scientific areas covered with these instruments since their introduction in 2018.

2 Zorro and ʻAlopeke: visiting speckle instruments at Gemini

ʻAlopeke and Zorro (the ʻōlelo Hawai'i and Spanish words for "fox") are identical instruments that use iXon Ultra 888 EMCCD cameras to provide simultaneous speckle imaging in two optical band passes, yielding high-resolution reconstructed images of the observed source. SDSS $u,g,r,i,z,H\alpha$, and 4 narrow-band filters are available in two filter wheels passing light dichorically split at 700 nm. These imagers are used with one of two circular fields-of-view: speckle mode (diameter = 6.7 arcseconds) or wide-field mode (diameter = 60 arcseconds). The left panel of Figure 1 shows ʻAlopeke with the covers removed, revealing the tightly packed innards that contain two filter wheels, the optical elements, and the two ANDOR EMCCD cameras extending from the box. The right panel of Figure 1 shows Zorro in its permanent mount location at the GCAL port, attached underneath the Gemini South 8.1-m primary mirror. The small space available for the speckle instruments did not allow for an atmospheric dispersion corrector (ADC) to be included. However, this exclusion is offset by the large advantage that our visitor instruments have in that they are permanently mounted on Gemini and therefore always available to use. We discuss our "no ADC" mitigation strategy below. A complete description of these two visiting Gemini instruments, including relative transmission as a function of wavelength in the 350–1,000 nm range, can be found in Scott et al. (2021) and at the Gemini Observatory instrument web pages[1].

ʻAlopeke and Zorro proposal demand at Gemini varies semester by semester, but on average it is 5%–10%, exceeding the Gemini South Adaptive Optics Imager (GSAOI) demand and nearing the demand for other visiting instruments (e.g., IGRINS), or even facility instruments (e.g., GNIRS). Any user can request time on these instruments using the regular Call for Proposals, or Director's Discretionary Time (DDT) when needed. Principal Investigators (PIs) from Gemini partner countries can also propose for ʻAlopeke and Zorro time using Fast Turnaround (FT) proposals[2].

3 Observations, data reduction, and image reconstruction

Speckle instrumentation is fairly simple, inexpensive, and small compared to other instruments mounted on large-aperture telescopes. ʻAlopeke and Zorro are roughly the size of a carry-on suitcase. The most difficult aspect of speckle observing is the quantity and short duration of the exposures, which is easily managed by the fast read-out capabilities of the EMCCDs. Using the Gemini mirror coating reflectivity, the optics and filter transmissions, and the QE of the EMCCDs, optimal speckle observations can be carried out between 400 and 940 nm where the total throughput is 40%

1 https://www.gemini.edu/instrumentation/alopeke-zorro

2 https://www.gemini.edu/observing/schedules-and-queue/

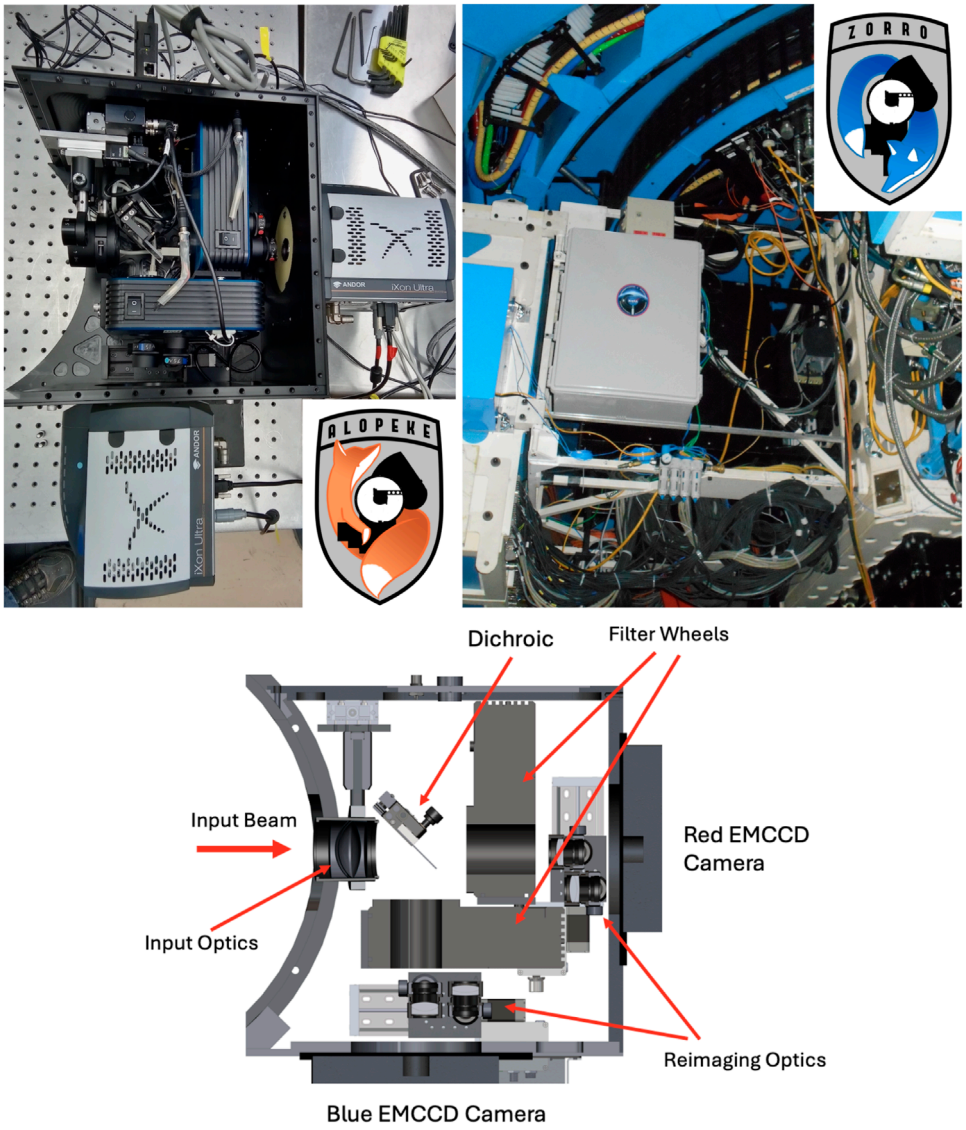

FIGURE 1
Top Left: The 'Alopeke main instrument components were visible during a routine maintenance inspection at the Gemini North base facility. The ANDOR EMCCD cameras are seen extending from the main enclosure. Top Right: Zorro mounted on the Gemini South telescope. The black box with one ANDOR camera seen extending from it contains the instrument, while the larger white box to the left contains the electronic power supplies and instrument computer. Bottom: Block Diagram of the speckle instrument with major parts labeled. See Scott et al. (2021) for complete instrument details.

or higher (Scott et al., 2021). As a mitigation for the lack of an ADC, typical speckle observations are performed at an airmass of 1.4–1.5 or lower (elevations above 45°) and narrow band filters are used. Speckle imaging at Gemini is often done under (bright) moonlit sky conditions, for which the narrow band filters are preferred as well. The EMCCDs can also function as normal CCDs, allowing traditional, long exposure digital images to be obtained.

Speckle imaging of a target requires many thousands of short exposures (10–60 ms in length) to be obtained and processed. This large number of images is required to build up sufficient S/N, especially at contrasts greater than four or five magnitudes ($\sim 10^{-2}$), at very close angular separations, and/or for fainter targets. Although this large number of exposures may seem daunting, at tens of milliseconds per image, typical speckle observations last only a few minutes per target (Hope et al., 2019; Howell and Furlan, 2022). Stars with V magnitudes from 1 to ~12 require only ~5 min of observation time, during which 3,000 to 5,000 thousand exposures are collected. However, targets as faint as $R = 19$ can be observed by using ~ 50 min of on-source time. In a typical night, 40 to 50 sources are observed. Scott et al. (2021) and Howell and Furlan (2022) provide full details on the relation between the magnitude of the source, the filter, the brightness of the target and the sky conditions to the total integration time at the source and the resulting S/N. To provide the reader with a gauge for the time required for a variety of observation types, we list in Section 5, the total on-source times and filters used for each observation.

Almost all currently used speckle image reconstruction software packages are based on Fourier speckle interferometric methods

(e.g., Labeyrie, 1970; Lohmann et al., 1983; Horch et al., 2001; Horch et al., 2015). Speckle imaging collects a highly magnified image of a source in a very short time period. Each collected image consists of numerous "speckles" that cover the area of the point spread function. A single speckle exposure therefore has little total flux, thus the need to obtain many individual short exposures, each sampling the atmospheric turbulence. Simply averaging the many exposures would yield just a native seeing image. Thus, the time averaged power spectrum is produced consisting of individual power spectra plus a transfer function of the combined telescope-atmosphere system. The transfer function can be evaluated by a separate measurement of a single point source (i.e., a PSF standard) allowing a solution for the target's power spectrum. Although this formulation can yield amplitude information on multiple sources or extended flux structures such as angular separations or magnitude differences, reconstructed images cannot be produced. To do so, the triple correlation or bi-spectrum technique is employed (Lohmann et al., 1983). A complete description of the speckle imaging process from observation through image reconstruction is beyond the scope of this short review paper, but is provided in detail in Beavers et al. (1989). The results presented in this paper, and all fully reduced data in the archives, are based on our implementation of the data reduction methods as described in Howell et al. (2011) and Horch et al. (2012). Our standard data reduction pipeline (Horch et al., 2012; Howell et al., 2011) provides robust 5σ magnitude contrast limits on stellar companion or circumstellar material detections (e.g., Howell et al., 2016). Speckle reconstructions scale the output image maximum value to 1.0 at the center of the image. All of the images presented in this paper (except Nova V906 Car and Eros which are shown using just a red intensity color map) have their brightest pixel scaled to 1.0 and are presented on a min-max log scale using the relative intensity colorbar shown in Figure 3.

Fourier speckle deconvolution techniques are computationally efficient but, as described above, require a PSF model power spectrum usually obtained via routine observation of stars taken from the HR or HD catalogs that are known or assumed to be single based on past spectroscopic or imaging observations. These PSF standards are assigned to each target by the observing team prior to the scheduled observations. They are observed near in time to the targets and with similar sky locations. Each PSF standard observation requires an additional ~3 minutes of observing time. Modern image reconstruction methods that are based on blind deconvolution techniques and can reach deeper contrasts plus provide more accurate astrophysical results are beginning to be implemented for speckle image reconstructions (e.g., Howell et al., 2024). Figure 2 presents a typical Gemini speckle imaging result for a point source (the star TOI-5873), and the discovery of a very close stellar companion that is 1.6 magnitudes fainter than the primary. Note the 180-degree autocorrelation quadrant ambiguity that occurs when stars have comparable brightness (Horch et al., 2012). During data reduction, a "best determination", using all sets of images taken of the target plus bispectrum analysis, is made to assign the correct location. The astrometric precision for binary stars observed at Gemini yields stellar separations to ±1 mas and ±1° in position angle (Lester et al., 2021). Photometric magnitude differences for stars in multiple systems typically have uncertainties of ±0.25 magnitudes, increasing by ~2× for very close or wide

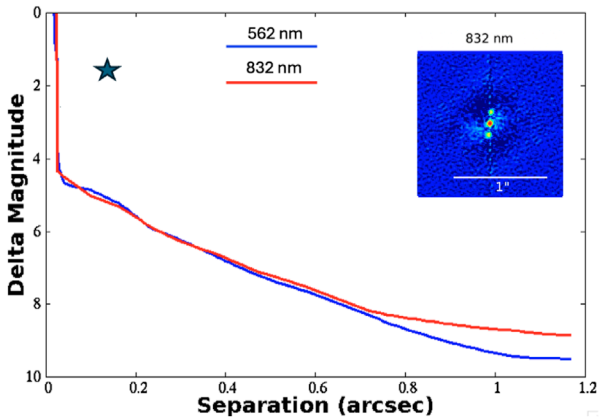

FIGURE 2
A typical speckle imaging result for an eighth magnitude star (TOI-5873). The red and blue curves show the 5σ contrasts achieved as a function of angular separation, from the diffraction limit out to 1.2 arcseconds. The star symbol shows the properties of the companion, and the inset shows the reconstructed image for the 832 nm observation; a scale bar is included for reference. The speckle observations revealed that the target star is binary, with a very close (0.14 arcsecond separation) companion that is 1.6 magnitudes fainter than the primary at position angle 176°. See §3 for details.

(> 0.9) pairs (e.g., Howell et al., 2011; Horch et al., 2012). Raw and fully reduced archival data from Zorro and 'Alopeke can be found in the Gemini Observatory (Hirst and Cardenes, 2017)[3] or Exoplanet Follow-up Observing Program[4] archives.

4 A panoply of scientific applications and results

In this section, we discuss various scientific targets that have been observed using 'Alopeke and/or Zorro. Most of these observations were obtained as test cases or engineering studies (unless otherwise noted) and as such, many have not been published previously. These studies allowed researchers to assess the potential for using speckle imaging to accomplish their scientific goals, and have formed the basis for a number of stand-alone proposals targeting the detailed study of single objects, or larger sample collection to enable more global results.

4.1 Stars

Stars have been the predominant targets of the speckle imaging campaigns. In this section, we explore the varied results from these observations.

3 https://archive.gemini.edu/searchform/ZORRO, https://archive.gemini.edu/searchform/ALOPEKE

4 https://exofop.ipac.caltech.edu/tess/

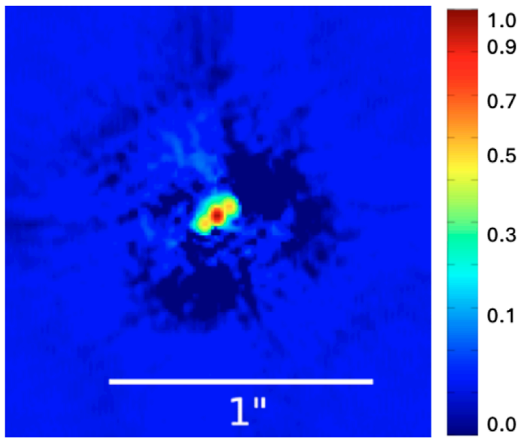

FIGURE 3
The microlens source Kojima-1Lb observed with 'Alopeke at Gemini North. This SDSS *i* band image was obtained using 35 min of on-source time and detected both the lens and source separated by 0.058 arcsec with a magnitude difference of 3.7. The very close (blended in the reconstructed image) companion shows a 180-degree ambiguity with the true source location being at P.A. = 110°. The colorbar shows the relative flux intensity for the image. North is up and East to the left in the image.

4.1.1 Exoplanet-hosting stars

Several large observing programs aimed at surveying exoplanet host stars have been in place at Gemini for many years. These programs have targeted transiting exoplanet candidates from Kepler, K2, TESS, and other NASA missions and have observed many thousands of stars (Lester et al., 2021; Howell et al., 2021a; 2021b; Clark et al., 2022; Matson et al. 2025). Such surveys aim to identify close-in stellar companions that either induce false positive signals or contaminate the light curves of planets, leading to underestimated planetary radii (Ciardi et al., 2015; Furlan and Howell, 2017). Figure 2 is an example of an eighth magnitude TESS exoplanet candidate host star observed at Gemini South with Zorro. Observations of exoplanet host stars continue for missions such as TESS, Roman, Ariel, and the Habitable Worlds Observatory. As the Roman space telescope prepares for launch, microlensing observations will reach a new high as numerous free-floating planets will be discovered via observations pointed toward the Galactic bulge. Speckle observations will play an important role in the resolution of the target star lens, as was done for the R~18 magnitude Kojima-1Lb microlens event (Figure 3).

4.1.2 Stellar multiplicity

Surveys investigating the multiplicity of various types of stars have been carried out at the Gemini Observatory. These include low-mass stars (e.g., Winters et al., 2021; Clark et al., 2022), halo stars, and higher-order multiplicity in known and metal-poor binaries (e.g., Hartman et al., 2022; Mendez et al., 2025). Figure 4 shows a faint likely L-dwarf companion to an M star identified by Deacon and Hambly (2007), as well as a newly discovered, planet-hosting triple star system TOI-697 (Lester et al., 2021). High-resolution imaging of triple star systems has been proposed as a robust test of modified gravity (Manchanda et al., 2023).

The space missions Kepler/K2 and TESS were designed to detect transiting exoplanets, but have also catalyzed a wealth of astrophysical discoveries. These findings include the detection of very high multiplicity stellar systems whose orbital planes are all edge-on to our line-of-sight. The speckle instruments at Gemini Observatory identified component stars in some of these doubly eclipsing quadruple systems and triply eclipsing triple systems (Kostov et al., 2024).

4.1.3 Angular diameters

Because speckle imaging allows the diffraction limit of the telescopes to be achieved, stars with large angular diameters can be resolved. 'Alopeke on Gemini North was used to observe Betelgeuse during its "Great Dimming Event" in February 2020. At the time, Betelgeuse had a *V* magnitude of 1.4. Figure 5 shows a 562 nm speckle image of the star along with an unresolved PSF reference star observed near in time. The angular resolution at 562 nm with the Gemini 8-m telescope is ~18 mas providing only ~2 resolution elements across the star, thus no details of the surface structure, such as super convection cells, could be obtained. The disk of Betelgeuse is resolved with an apparent angular diameter of 40 mas.

4.1.4 Stellar eclipses

Stepping aside from speckle interferometry for just a moment, we provide an example showcasing the ability for the rapid readout EMCCDs to be used as normal digital imagers with the ability to collect fast time series observations of temporally changing sources. Figure 6 shows a SDSS *i* light curve of the r = 18 magnitude eclipsing double degenerate binary star SDSS J0822+3048 with a period of 40.5 min (Kosakowski et al., 2021). Time series standard CCD observations, comprised of 15-s exposures, were simultaneously obtained in SDSS *r* and SDSS *i* for about 2 h, allowing the very short, 90-s duration eclipse to be examined in detail.

4.1.5 Evolved stars and stellar remnants

As stars end their lives, they often eject material into space either as soft puffs of atmospheric material or the rapid energetic explosion of a supernova. These sources often consist of a central point-source-like object surrounded by symmetric or very asymmetric material outflows (see, e.g., Huang et al., 2023). Evolved stars–such as interacting binary systems, common envelope pairs, and symbiotic stars–can often show resolved features as well.

Speckle observations have allowed the measurement of winds from Wolf-Rayet stars (Shara et al., 2023), shapes of stellar merger remnants (Mobeen et al., 2024), nova shells (Figure 7), supernovae (Van Dyket al., 2024) and well-known specific targets such as R Aqr and Eta Carinae (Figure 8). Eta Car was first observed with speckle imaging by Weigelt and Ebersberger (1986) who found four starlike components in their field of view of 0.8". The Gemini speckle image shown in (Figure 8) reveals the central light concentration and fans of extended wind emission coming from the binary.

4.2 Solar system bodies

Speckle imaging is also useful for objects in our own backyard. This section presents observations of Solar System objects.

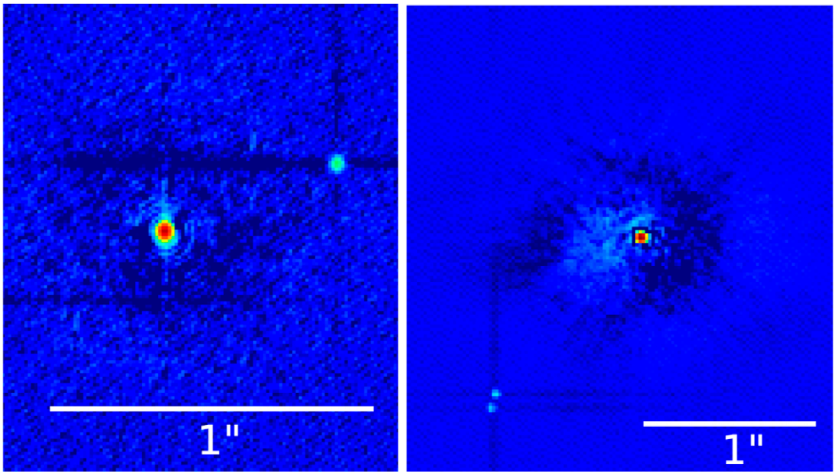

FIGURE 4
Left: The late M star WISE J133734.15-371100.2 as observed by Zorro. This ninth magnitude star was observed for 30 min at 832 nm. Note the close companion at a separation of 0.6 arcsec that is three magnitudes fainter. At a distance of 34 pc, the two stars are 20 au apart and have masses of 0.23 and 0.09 $M_{\odot}$ respectively. Right: The planet hosting star TOI-697 was discovered to be triple using Gemini speckle observations. The primary star harbors a 2.6 $R_{\oplus}$ planet in a 8.6 days orbit and is itself orbited by a close binary pair five magnitudes fainter at a separation of 1.15 arcsec (Armstrong et al., 2025). This 832 nm observation used 5 min of Gemini time.

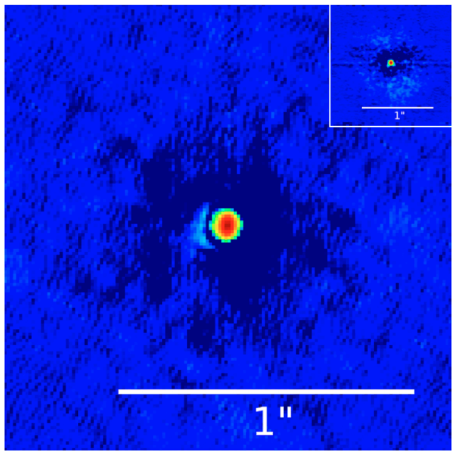

FIGURE 5
A 562 nm 'Alopeke observation of Betelgeuse obtained in February 2020, during the "Great Dimming Event." Betelgeuse, $V = 1.4$, is resolved with an angular diameter of 40 mas. The inset shows an unresolved diffraction limited PSF reference star observed near in time to Betelgeuse. This observation took a total of 12 min of Gemini time.

4.2.1 Angular sizes

Many objects in our Solar System are large enough to be resolved. Speckle images of Pluto and Charon provided measurements of their diameters, and were the highest resolution images of the (dwarf) planets until the New Horizons fly-by (Howell et al., 2012). Asteroids have also been targets of the Gemini speckle imagers. During its close approach, the asteroid Phaethon (1983 TB) was found to be 59 mas in angular size, corresponding to a physical size of 4.1 km (Wooden et al., 2018). Pereira et al. (2023) observed a stellar occultation by the Trans-Neptunian object Quaoar with the aim of improving its shape model and physical parameters and searching for additional material around the body. Figure 9 shows five frames from a 5.3-h speckle imaging observation sequence of the asteroid 433 Eros. Eros is the second largest near-Earth asteroid. It has an elongated shape and a volume equivalent diameter of ~17 km. The time series covered a single rotation period (P = 5.3 h) of the asteroid, and the apparent shape of the non-spherical body is seen to change with time. These data are unpublished and available in the Gemini archive.

4.2.2 Occultations

Pluto, asteroids, Kuiper Belt Objects, and other Solar System bodies have also had occultations observed by the Gemini speckle imagers, using simultaneous high-speed two-color photometry (e.g., Sickafoose et al., 2023). Other studies have observed target stars in advance of an occultation to assess whether they are single or multiple (e.g., Schindler et al., 2019).

4.3 Extragalactic sources and eruptive events

This last section presents several Gemini speckle imaging programs related to celestial objects that "go bang in the night" and require fast action to observe the start of their eruptions, and/or fast sampling to reveal rapidly evolving structures in their light curves.

4.3.1 Crowded fields

The black hole binary V4641 Sgr is in an extremely crowded field (Figure 10). Speckle observations provided not only a precise location of the source, but unblended photometric measurements as well. Speckle imaging has also been used in crowded regions of the

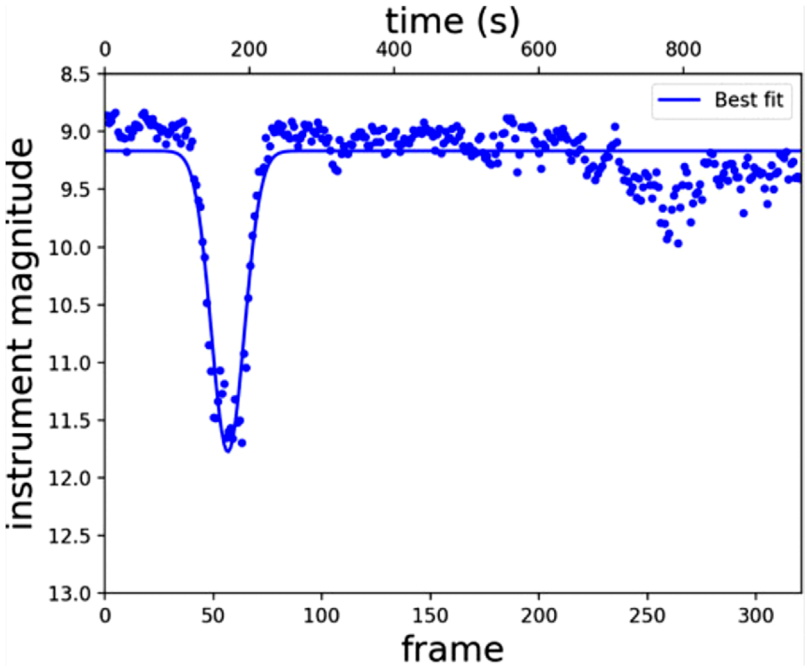

FIGURE 6
Photometric eclipse light curve in SDSS *i* of the double degenerate binary star SDSS J0822+3048. The time series consisted of 2 h of 15 s exposures that were used to provide ingress and egress details for the short eclipse. Adapted from Scott et al. (2021).

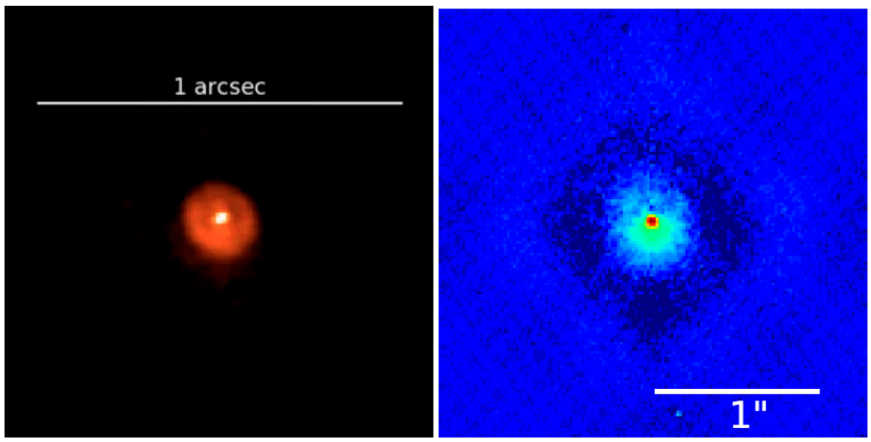

FIGURE 7
Speckle images of resolved nova shells. Left: Nova V906 Car observed in November 2020, 978 days after its explosion. The image was taken at 832 nm and shows a resolved nova shell with a radius of 90 mas. Right: The classical nova V603 Aql (Nova Aql 1918) shows an asymmetric inner shell at 832 nm. The full extent of the gas shell of V603 Aql is near 100 arcsec, while this speckle image reveals an inner continuum emitting (dust?) shell of ~0.5 arcsec in extent. Each of these observations used 20 min of Gemini time.

Magellanic Clouds to search for binaries and resolve the core of R136 (Kalari et al., 2022; Kalari et al., 2024).

4.3.2 Dual quasars

Observation of a 19th magnitude dual quasar candidate resulted in the detection of both binary black hole nuclei, and required only 50 min of Gemini time (Howell et al., 2021c). Earlier speckle interferometry imaging observations for quasars, even with 6-m telescopes, were limited to brighter (≤16) targets. New speckle observations with Gemini allow nearly diffraction-limited optical imaging opening a new venue to the confirmation and detailed studies of high-z dual quasars.

4.3.3 X-ray binary outbursts

Outbursts of X-ray binaries offer opportunities to measure quasi-periodic oscillations during the accretion process, yielding

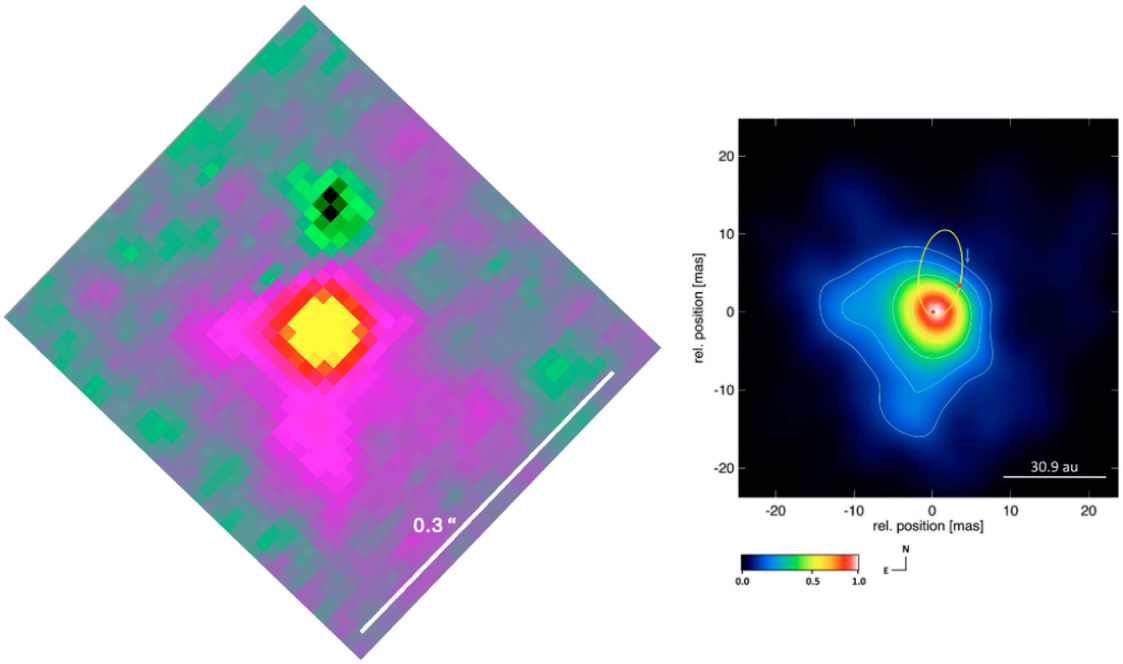

FIGURE 8
Two images of the famous star Eta Carina. Left: A false color composite composed of summed speckle images in the SDSS *u*, 562 nm, and 832 nm filters. These observations used a total of 40 min of Gemini time. The speckle image is ~0.3 arcseconds (300 mas) on a side. Right: The highest resolution image of Eta Car available today covering the inner 50 mas around the binary. This image was made using the ESO VLTI AMBER instrument in the K band (Weigelt et al., 2016). The orbit of the secondary star around the primary is shown for comparison. The VLTI image contours outline the K band continuum wind emission which is seen to extend to larger distances in the optical speckle composite image.

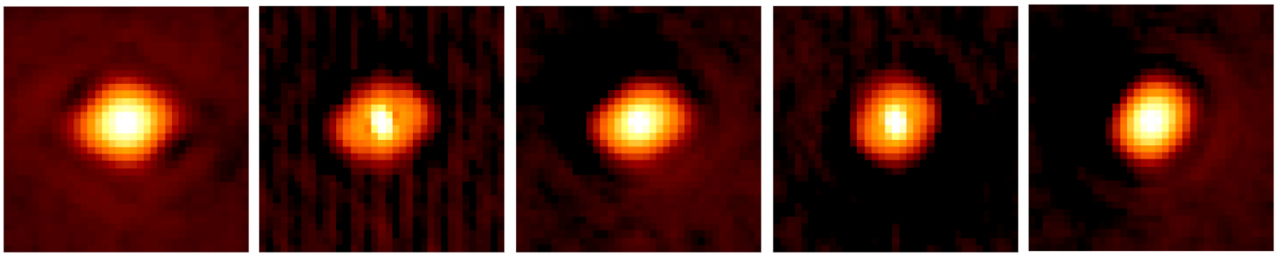

FIGURE 9
Selected frames from a speckle imaging time series of the asteroid Eros that covered roughly one rotation period (5.3 h). These 832 nm data were obtained in February 2020 at the Gemini South telescope using Zorro, and the time series data were reduced as 25 reconstructed images, each using five sets of 1000 × 60 millisecond exposures and requiring ~12 min of Gemini time. During the series, the apparent shape of the non-spherical body is seen changing with time.

insights into the underlying disks. Tetarenko et al. (2022) used speckle imaging to perform an optical fast timing study of various X-ray binaries. The simultaneous two-color data collected enabled the examination of disk energetics and jet physics. Furthermore, Scott et al. (2018) showed, using engineering data from the WIYN telescope, that the ability to detect both pulse shape and pulse period in two optical colors at the same time allows precise identification of the pulsational modes involved in the pulsating white dwarf HL Tau.

4.3.4 Fast radio bursts

Fast radio bursts (FRB) are mysterious transient sources. FRB 20180916B repeats with a known period, making it a useful test case. Kilpatrick et al. (2024) used ʻAlopeke to observe FRB 20180916B simultaneously in the SDSS *r* and SDSS *i* bands, requiring 20 min of Gemini time. No optical burst was detected at the time of the radio burst, allowing certain FRB models to be ruled out.

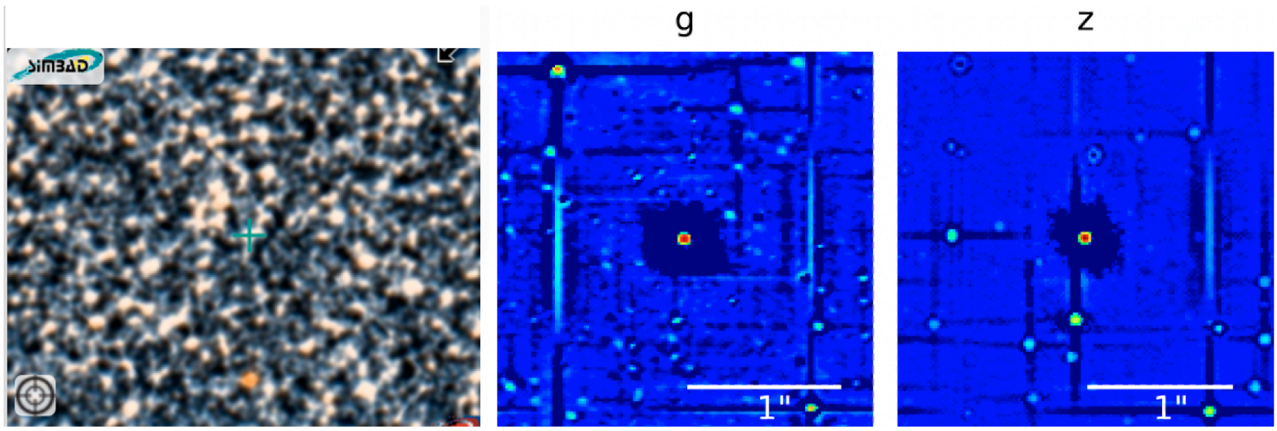

FIGURE 10
V4641 Sgr, a $V \sim 14$, high-mass black hole binary, is easily isolated from its very crowded field in speckle images. *Left:* A DSS image showing a 4×4 arcminute region around V4641 Sgr (from SIMBAD). *Right:* Simultaneous SDSS *g* and SDSS *z* speckle images for which photometry can be performed without issues of crowding. These images were obtained using 'Alopeke and 12 min of Gemini time.

5 Summary

The 'Alopeke and Zorro speckle cameras are permanent visitor instruments at the Gemini North and South telescopes in Hawai'i and Chile. One can request to use these instruments for general queue proposals, DDT and FT proposals, Long and Large Proposals, and Target of Opportunity proposals as well. Note that the oversubscription rate of the Gemini telescopes hovers near 3, as compared to 6–7 for HST, Chandra, and JWST.

Optical speckle imaging has the advantage of darker skies (than the IR), no need for AO natural or laser guide stars, inexpensive and simple instrumentation, and easy setup and use. Gemini speckle observations can be made from 350 nm to 1,000 nm, providing the ability to gather a spectral energy distribution across the optical bandpass for any detected companion. Additionally, speckle imaging reaches the diffraction limit and is indifferent to whether the target star is single or multiple; the observations and data reduction processes are uniformly applied regardless of the target's multiplicity. This is not an ability shared by coronagraphic instruments.

The applications of speckle imaging have broadened greatly since 'Alopeke and Zorro were first installed at Gemini Observatory. While first used to observe stars at high angular resolution to search for stellar companions, speckle imaging is now employed to decipher the shape of Solar System bodies, study the outflows and ejected material of supernova, observe extragalactic eruptive events, and investigate other exciting astrophysical phenomena.

As the world of ground-based observational astronomy moves into the era of 30–40 m-class telescopes, speckle imagers should be one of the first facility instruments available. Speckle imagers are inexpensive, simple to construct, small in format, light in weight, and easy to operate. The use of EMCCDs and their high-speed imaging ability not only allows speckle imaging to be accomplished but fast time-series photometric observations as well. Such time-series observations of bright stars can also find telescope engineering applications in the analysis of x,y centroids over time to examine guider and tracking errors, and unwanted telescope vibration modes. This type of engineering study has already been successfully implimented at Gemini using 'Alopeke and Zorro. The high-speed imaging cameras can also be used as telescope guiders or wavefront sensors, such as has been done at the WIYN telescope for use with the NEID spectrograph (see, e.g., Gupta et al., 2021).

Speckle instrument imagers can also function as standard CCD imagers. Providing, as we have in 'Alopeke and Zorro, an optional wider field of view, the EMCCD cameras can be used as conventional CCD imagers, providing long-exposure photometric images. As a "first-light" instrument, obtaining images throughout the larger final field of view would yield optical quality checks of the delivered PSF across the focal plane.

As speckle interferometry moves to these larger telescopes, reaching the optical diffraction limit on a 30-m-class telescope would provide, at 400 nm, an spectacular ground-based angular resolution of 4 mas. Such imaging resolution would be fantastic, allowing a multitude of new astrophysical science cases to be explored.

Author contributions

SH: Conceptualization, Funding acquisition, Methodology, Project administration, Validation, Writing – original draft, Writing – review and editing. CM-V: Conceptualization, Methodology, Validation, Writing – original draft, Writing – review and editing. EF: Formal Analysis, Software, Validation, Writing – review and editing. NS: Data curation, Software, Writing – review and editing. RM: Data curation, Validation, Writing – review and editing. CL: Formal Analysis, Software, Validation, Writing – review and editing. CC: Data curation, Formal Analysis, Software, Writing – review and editing. KL: Formal Analysis, Validation, Writing – review and editing. ZH: Formal Analysis, Validation, Writing – review and editing. DC: Funding acquisition, Project administration, Writing

– review and editing. SD: Data curation, Software, Writing – review and editing.

Funding

The author(s) declare that financial support was received for the research and/or publication of this article. Funding for this work has been provided by the NASA Exoplanet Program Office and NASA headquarters.

Acknowledgments

We would like to acknowledge the staff at the international Gemini Observatory for their many hours of support, help, and friendship that allowed this high-resolution imaging to be possible. Science Operation Specialists, contact scientists, and queue coordinators have been particularly supportive and patient with us during our programs. We also appreciate the allocations of engineering time that allowed us to test various observational modes and increase community service. An especially big thanks to Mark Everett, Dave Mills, Rebecca Gore, Sergio Fajardo-Acosta, Andy Adamson, Jeong-Eun Heo, Atsuko Nitta, Fredrik Rantakyro, Joanna Thomas-Osip, Venu Kalari, Ricardo Salinas, Andrew Stephens, and John White. The authors also thank the American Astronomical Society for organizing meetings with poster and free-time community gatherings that promote friendly and productive conversations that can turn into interesting research and publications such as this paper. The observations in this paper made use of the High-Resolution Imaging instruments ʻAlopeke and Zorro. ʻAlopeke and Zorro were funded by the NASA Exoplanet Exploration Program and built at the NASA Ames Research Center by Steve B. Howell, Nic Scott, Elliott P. Horch, and Emmett Quigley. ʻAlopeke and Zorro are mounted on both 8.1-m telescopes of the international Gemini Observatory, a program of NSF NOIRLab, which is managed by the Association of Universities for Research in Astronomy (AURA) under a cooperative agreement with the U.S. National Science Foundation, on behalf of the Gemini partnership: the National Science Foundation (United States), National Research Council (Canada), Agencia Nacional de Investigación y Desarrollo (Chile), Ministerio de Ciencia, Tecnología e Innovación (Argentina), Ministério da Ciência, Tecnologia, Inovações e Comunicações (Brazil), and Korea Astronomy and Space Science Institute (Republic of Korea). This research has made use of the NASA Exoplanet Archive and ExoFOP, which are operated by the California Institute of Technology, under contract with the National Aeronautics and Space Administration under the Exoplanet Exploration Program. Additional information was obtained from the SIMBAD database, operated at CDS, Strasbourg, France. We acknowledge support from AFOSR awards FA9550-14-1-0178 (DAH and SMJ) and FA9550-21-1-0384 (SMJ). *Facilities:* Gemini - ʻAlopeke, Zorro.

Conflict of interest

The authors declare that the research was conducted in the absence of any commercial or financial relationships that could be construed as a potential conflict of interest.

The author(s) declared that they were an editorial board member of Frontiers, at the time of submission. This had no impact on the peer review process and the final decision.

Generative AI statement

The author(s) declare that no Generative AI was used in the creation of this manuscript.

Publisher's note

References

Armstrong, D. J., Osborn, A., Burn, R., Venturini, J., Adibekyan, V., Bonfanti, A., et al. (2025). The NCORES programme: precise planetary masses, null results, and insight into the planet mass distribution near the radius gap. *MNRAS* 537, 3175–3193. doi:10.1093/mnras/staf175

Balega, I. I., Balega, Y. Y., Belkin, I. N., Vasyuk, V. A., and Maksimov, A. F. (1993). Television speckle interferometry of binary stars at the Zeiss-1000 telescope. *Bull. Special Astrophysics Observatory* 35, 9–14. Available online at: https://ui.adsabs.harvard.edu/abs/1993BSAO...35....9B.

Beavers, W. I., Dudgeon, D. E., Beletic, J. W., and Lane, M. T. (1989). Speckle imaging through the atmosphere. *Linc. Laboratory J.* 2, 207–228. Available online at: https://ui.adsabs.harvard.edu/abs/1989LLabJ...2..207B.

Bonneau, D., and Foy, R. (1980). Speckle interferometric observations of binary systems with the Hte-Provence 1.93 M telescope. *A&A* 86, 295–298. Available online at: https://ui.adsabs.harvard.edu/abs/1980A&A....86..295B.

Ciardi, D. R., Beichman, C. A., Horch, E. P., and Howell, S. B. (2015). Understanding the effects of stellar multiplicity on the derived planet radii from transit surveys: implications for kepler, K2, and TESS. *ApJ* 805, 16. doi:10.1088/0004-637x/805/1/16

Clark, C. A., van Belle, G. T., Ciardi, D. R., Lund, M. B., Howell, S. B., Everett, M. E., et al. (2022). A dearth of close-in stellar companions to M-dwarf TESS objects of interest. *AJ* 163, 232. doi:10.3847/1538-3881/ac6101

Clark, C. A., van Belle, G. T., Horch, E. P., Trilling, D. E., Hartman, Z. D., Collins, M., et al. (2020). "The optomechanical design of the quad-camera wavefront-sensing six-channel speckle interferometer (QWSSI)," in *Society of photo-optical instrumentation engineers (SPIE) conference series. Vol. 11446 of society of photo-optical instrumentation engineers (SPIE) conference series*.

Deacon, N. R., and Hambly, N. C. (2007). Southern infrared proper motion survey. II. A sample of low mass stars with $\mu \geq 0.1$/yr. *A&A* 468, 163–170. doi:10.1051/0004-6361:20066844468163D

Fried, D. L. (1966). Limiting resolution looking down through the atmosphere. *J. Opt. Soc. Am. (1917-1983)* 56, 1380–1456. doi:10.1364/josa.56.001380

Furlan, E., and Howell, S. B. (2017). The densities of planets in multiple stellar systems. *AJ* 154, 66. doi:10.3847/1538-3881/aa7b70

Gupta, A. F., Wright, J. T., Robertson, P., Halverson, S., Luhn, J., Roy, A., et al. (2021). Target prioritization and observing strategies for the NEID earth twin survey. *AJ* 161, 130. doi:10.3847/1538-3881/abd79e

Hartkopf, W. I., Mason, B. D., McAlister, H. A., Roberts, J., Lewis, C., Turner, N. H., et al. (2000). ICCD speckle observations of binary stars. XXIII. Measurements during 1982-1997 from six telescopes, with 14 new orbits. *AJ* 119, 3084–3111. doi:10.1086/301402

Hartman, Z. D., Lépine, S., and Medan, I. (2022). Vetting the "lobster" Diagram: searching for unseen companions in wide binaries using NASA space exoplanet missions. *ApJ* 934, 72. doi:10.3847/1538-4357/ac72a0

Hirst, P., and Cardenes, R. (2017). A new data archive for Gemini - fast, cheap and in the cloud. In *Astronomical data analysis software and systems XXV*, eds N. P. F. Lorente, K. Shortridge, and R. Wayth (Provo, Utah: Brigham Young University) 512, 53.

Hope, D., Jefferies, S., Li Causi, G., Stangalini, M., Pedichini, F., Mattioli, M., et al. (2019). "High-resolution imaging of closely space objects with high contrast ratios," in *Advanced maui optical and space surveillance technologies conference*.

Hope, D. A., Jefferies, S. M., Li Causi, G., Landoni, M., Stangalini, M., Pedichini, F., et al. (2022). Post-AO high-resolution imaging using the kraken multi-frame blind deconvolution algorithm. *ApJ* 926, 88. doi:10.3847/1538-4357/ac2df3

Horch, E., Franz, O. G., and Ninkov, Z. (2000). CCD speckle observations of binary stars from the southern hemisphere. II. Measures from the lowell-tololo telescope during 1999. *AJ* 120, 2638–2648. doi:10.1086/316826

Horch, E., Morgan, J. S., Giaretta, G., and Kasle, D. B. (1992). A new speckle interferometry system for the MAMA detector. *PASP* 104, 939. doi:10.1086/133078

Horch, E., Ninkov, Z., and Franz, O. G. (2001). CCD speckle observations of binary stars from the southern hemisphere. III. Differential photometry. *AJ* 121, 1583–1596. doi:10.1086/319423

Horch, E. P., Howell, S. B., Everett, M. E., and Ciardi, D. R. (2012). Observations of binary stars with the differential speckle survey instrument. IV. Observations of kepler, CoRoT, and hipparcos stars from the Gemini North telescope. *AJ* 144, 165. doi:10.1088/0004-6256/144/6/165

Horch, E. P., van Altena, W. F., Demarque, P., Howell, S. B., Everett, M. E., Ciardi, D. R., et al. (2015). Observations of binary stars with the differential speckle survey instrument. V. Toward an empirical metal-poor mass-luminosity relation. *AJ* 149, 151. doi:10.1088/0004-6256/149/5/151

Horch, E. P., van Altena, W. F., Howell, S. B., Sherry, W. H., and Ciardi, D. R. (2011). Observations of binary stars with the differential speckle survey instrument. III. Measures below the diffraction limit of the WIYN telescope. *AJ* 141, 180. doi:10.1088/0004-6256/141/6/180

Howell, S. B., Everett, M. E., Horch, E. P., Winters, J. G., Hirsch, L., Nusdeo, D., et al. (2016). Speckle imaging excludes low-mass companions orbiting the exoplanet host star TRAPPIST-1. *ApJ* 829, L2. doi:10.3847/2041-8205/829/1/L2

Howell, S. B., Everett, M. E., Sherry, W., Horch, E., and Ciardi, D. R. (2011). Speckle camera observations for the NASA kepler mission follow-up program. *AJ* 142, 19. doi:10.1088/0004-6256/142/1/19

Howell, S. B., and Furlan, E. (2022). Speckle interferometric observations with the Gemini 8-m telescopes: signal-to-noise calculations and observational results. *Front. Astronomy Space Sci.* 9, 871163. doi:10.3389/fspas.2022.871163

Howell, S. B., Horch, E. P., Everett, M. E., and Ciardi, D. R. (2012). Speckle camera imaging of the planet Pluto. *PASP* 124, 1124–1131. doi:10.1086/668405

Howell, S. B., Martinez, A. O., Hope, D. A., Ciardi, D. R., Jefferies, S. M., Baron, F. R., et al. (2024). High-contrast, high-angular-resolution optical speckle imaging: uncovering hidden stellar companions. *AJ* 167, 258. doi:10.3847/1538-3881/ad3df2

Howell, S. B., Matson, R. A., Ciardi, D. R., Everett, M. E., Livingston, J. H., Scott, N. J., et al. (2021a). Speckle observations of TESS exoplanet host stars: understanding the binary exoplanet host star orbital period distribution. *AJ* 161, 164. doi:10.3847/1538-3881/abdec6

Howell, S. B., Scott, N. J., Matson, R. A., Everett, M. E., Furlan, E., Gnilka, C. L., et al. (2021b). The NASA high-resolution speckle interferometric imaging program: validation and characterization of exoplanets and their stellar hosts. *Front. Astronomy Space Sci.* 8, 10. doi:10.3389/fspas.2021.635864

Howell, S. B., Shen, Y., Furlan, E., Gnilka, C. L., and Stephens, A. W. (2021c). Gemini speckle imaging of dual quasar candidates. *Res. Notes Am. Astronomical Soc.* 5, 210. doi:10.3847/2515-5172/ac26c8

Huang, C. D., Karovska, M., Hack, W., Raymond, J. C., Montez, R., and Kashyap, V. L. (2023). Shocks and Photoionization of the Inner 650 au Jet of the Interacting Binary Star R Aquarii from Multiwavelength Hubble Space Telescope Observations. *ApJ* 947, 11. doi:10.3847/1538-4357/acc068

Kalari, V. M., Horch, E. P., Salinas, R., Vink, J. S., Andersen, M., Bestenlehner, J. M., et al. (2022). Resolving the core of R136 in the optical. *ApJ* 935, 162. doi:10.3847/1538-4357/ac8424

Kalari, V. M., Salinas, R., Zinnecker, H., Rubio, M., Herczeg, G., and Andersen, M. (2024). A high-resolution imaging survey of massive young stellar objects in the magellanic Clouds. *ApJ* 972, 3. doi:10.3847/1538-4357/ad5bd9

Kilpatrick, C. D., Tejos, N., Andersen, B. C., Prochaska, J. X., Núñez, C., Fonseca, E., et al. (2024). Limits on optical counterparts to the repeating fast radio burst 20180916B from high-speed imaging with gemini-north/'alopeke. *ApJ* 964, 121. doi:10.3847/1538-4357/ad2687

Kosakowski, A., Kilic, M., and Brown, W. (2021). Multiband light-curve analysis of the 40.5-min period eclipsing double-degenerate binary SDSS J082239.54+304857.19. *MNRAS* 500, 5098–5105. doi:10.1093/mnras/staa3571

Kostov, V. B., Rappaport, S. A., Borkovits, T., Powell, B. P., Gagliano, R., Omohundro, M., et al. (2024). TIC 290061484: a triply eclipsing triple system with the shortest known outer period of 24.5 days. *ApJ* 974, 25. doi:10.3847/1538-4357/ad7368

Labeyrie, A. (1970). Attainment of diffraction limited resolution in large telescopes by fourier analysing speckle patterns in star images. *A&A* 6, 85. Available online at: https://ui.adsabs.harvard.edu/abs/1970A&A.....6...85L.

Lester, K. V., Matson, R. A., Howell, S. B., Furlan, E., Gnilka, C. L., Scott, N. J., et al. (2021). Speckle Observations of TESS Exoplanet Host Stars. II. Stellar Companions at 1-1000 au and Implications for Small Planet Detection. *AJ* 162, 75. doi:10.3847/1538-3881/ac0d06

Lohmann, A. W., Weigelt, G., and Wirnitzer, B. (1983). Speckle masking in astronomy: triple correlation theory and applications. *Appl. Opt.* 22, 4028–4037. doi:10.1364/AO.22.004028

Maksimov, A. F., Balega, Y. Y., Dyachenko, V. V., Malogolovets, E. V., Rastegaev, D. A., and Semernikov, E. A. (2009). The EMCCD-based speckle interferometer of the BTA 6-m telescope: description and first results. *Astrophys. Bull.* 64, 296–307. doi:10.1134/S1990341309030092

Manchanda, D., Sutherland, W., and Pittordis, C. (2023). Wide Binaries as a Modified Gravity test: prospects for detecting triple-system contamination. *Open J. Astrophysics* 6, E2. doi:10.21105/astro.2210.07781

Mason, B. D., ten Brummelaar, T., Gies, D. R., Hartkopf, W. I., and Thaller, M. L. (1997). ICCD speckle observations of binary stars.XVIII.an investigation of Be =. *AJ* 114, 2112. doi:10.1086/118630

Matson, R. A., Gore, R., Howell, S. B., Ciardi, D. R., Christiansen, J. L., Clark, C. A., et al. (2025). Demographics of M Dwarf binary exoplanet hosts discovered by TESS. *AJ* 169, 76. doi:10.3847/1538-3881/ad9923

McAlister, H. A., Hartkopf, W. I., Hutter, D. J., Shara, M. M., and Franz, O. G. (1987). ICCD speckle observations of binary stars. I. A survey for duplicity among the bright stars. *AJ* 93, 183. doi:10.1086/114297

McAlister, H. A., Hartkopf, W. I., Sowell, J. R., Dombrowski, E. G., and Franz, O. G. (1989). ICCD speckle observations of binary stars. IV. Measurements during 1986-1988 from the kitt peak 4-m telescope. *AJ* 97, 510. doi:10.1086/115001

Mendez, R. A., Tokovinin, A., Costa, E., and Dirk, M. (2025). Southern binaries with the Zorro speckle camera @ gemini-south. *arXiv e-prints*, 08721. doi:10.48550/arXiv.2503.08721

Mobeen, M. Z., Kamiński, T., Matter, A., Wittkowski, M., Monnier, J. D., Kraus, S., et al. (2024). Reconstructing the near-to mid-infrared environment in the stellar merger remnant V838 Monocerotis. *A&A* 686, A260. doi:10.1051/0004-6361/202347322686A.260M

Pedichini, F., Ambrosino, F., Centrone, M., Farinato, J., Li Causi, G., Pinna, E., et al. (2016). The V-SHARK high contrast imager at LBT. In *Ground-based and airborne instrumentation for astronomy VI*, eds C. J. Evans, L. Simard, and H. Takami (Washington, DC: Society of Photo-Optical Instrumentation Engineers (SPIE) Conference Series) 9908, 990832.

Pereira, C. L., Sicardy, B., Morgado, B. E., Braga-Ribas, F., Fernández-Valenzuela, E., Souami, D., et al. (2023). The two rings of (50000) Quaoar. *A&A* 673, L4. doi:10.1051/0004-6361/202346365673L4P

Salinas, R., Hajdu, G., Prudil, Z., Howell, S., and Catelan, M. (2020). A speckle interferometric search for a companion to the RR lyrae star UV oct. *Res. Notes Am. Astronomical Soc.* 4, 143. doi:10.3847/2515-5172/abb022

Schindler, K., Bosh, A. S., Levine, S. E., Person, M. J., Wolf, J., Zuluaga, C., et al. (2019). Results from a stellar occultation by KBO Varda. *AGU Fall Meet. Abstr.* 2019, P42C–P08. Available online at: https://ui.adsabs.harvard.edu/abs/2019AGUFM.P42C..08S.

Scott, N. J., Howell, S. B., Gnilka, C. L., Stephens, A. W., Salinas, R., Matson, R. A., et al. (2021). Twin high-resolution, high-speed imagers for the Gemini telescopes: instrument description and science verification results. *Front. Astronomy Space Sci.* 8, 138. doi:10.3389/fspas.2021.716560

Scott, N. J., Howell, S. B., Horch, E. P., and Everett, M. E. (2018). The NN-explore exoplanet stellar speckle imager: instrument description and preliminary results. *PASP* 130, 054502. doi:10.1088/1538-3873/aab484

Shara, M. M., Howell, S. B., Furlan, E., Garland, J. T., Moffat, A. F. J., and Zurek, D. (2023). Speckle imaging of γ^2 Velorum: the inner wind possibly resolved. *MNRAS* 525, 3195–3200. doi:10.1093/mnras/stad2482

Shara, M. M., Howell, S. B., Furlan, E., Gnilka, C. L., Moffat, A. F. J., Scott, N. J., et al. (2022). A speckle-imaging search for close and very faint companions to the nearest and brightest Wolf-Rayet stars. *MNRAS* 509, 2897–2907. doi:10.1093/mnras/stab2666

Sickafoose, A., Person, M., Zuluaga, C., Bosh, A., Levine, S., Brothers, T., et al. (2023). Pluto's atmosphere persists. In *AAS/Division for planetary sciences meeting abstracts #55* (Houston, TX: AAS/Division for Planetary Sciences Meeting Abstracts) 55.

Tetarenko, A., Maccarone, T., Vincentelli, F., Casella, P., Miller-Jones, J., Gandhi, P., et al. (2022). Optical fast timing observations of X-ray binaries with gemini's 'alopeke and Zorro. *44th COSPAR Sci. Assem. Held 16-24 July* 44, 1750. Available online at: https://ui.adsabs.harvard.edu/abs/2022cosp...44.1750T.

Tokovinin, A., and Cantarutti, R. (2008). First speckle interferometry at SOAR telescope with electron-multiplication CCD. *PASP* 120, 170–177. doi:10.1086/528809

Tokovinin, A., Cantarutti, R., Tighe, R., Schurter, P., van der Bliek, N., Martinez, M., et al. (2010). High-resolution imaging at the SOAR telescope. *PASP* 122, 1483–1494. doi:10.1086/657903

Van Dyk, S. D., Srinivasan, S., Andrews, J. E., Soraisam, M., Szalai, T., Howell, S. B., et al. (2024). The SN 2023ixf progenitor in M101. II. Properties. *ApJ* 968, 27. doi:10.3847/1538-4357/ad414b

Weigelt, G., and Baier, G. (1985). R 136a in the 30 Doradus nebula resolved by holographic speckle interferometry. *A&A* 150, L18–L20. Available online at: https://ui.adsabs.harvard.edu/abs/1985A&A...150L..18W.

Weigelt, G., and Ebersberger, J. (1986). Eta Carinae resolved by speckle interferometry. *A&A* 163, L5–L6 163L. Available online at: https://ui.adsabs.harvard.edu/abs/1986A&A...163L...5W.

Weigelt, G., Hofmann, K. H., Schertl, D., Clementel, N., Corcoran, M. F., Damineli, A., et al. (2016). VLTI-AMBER velocity-resolved aperture-synthesis imaging of η Carinae with a spectral resolution of 12 000. Studies of the primary star wind and innermost wind-wind collision zone. *A&A* 594, A106. doi:10.1051/0004-6361/201628832594A.106W

Weigelt, G. P. (1977). Modified astronomical speckle interferometry "speckle masking". *Opt. Commun.* 21, 55–59. doi:10.1016/0030-4018(77)90077-3

Winters, J. G., Charbonneau, D., Henry, T. J., Irwin, J. M., Jao, W.-C., Riedel, A. R., et al. (2021). The volume-complete sample of M dwarfs with masses $0.1 \leq M/M_{\odot} \leq 0.3$ within 15 parsecs. *Aj. 161* 161, 63. doi:10.3847/1538-3881/abcc74

Wooden, D. H., Dotson, J. L., Howell, S. B., and Horch, E. P. (2018). "Direct imaging of near earth object 3200 Phaethon (1983 TB)," in *49th annual lunar and planetary science conference. Lunar and planetary science conference, 1919*.